Journal of Environmental Radioactivity 203 (2019) 179–186

Contents lists available at ScienceDirect

Journal of Environmental Radioactivity

journal homepage: www.elsevier.com/locate/jenvrad

Uranium biosorption by *Lemna* sp. and *Pistia stratiotes*

Ludmila Cabreira Vieira[a], Leandro Goulart de Araujo[b,*], Rafael Vicente de Padua Ferreira[b], Edson Antonio da Silva[c], Rafael Luan Sehn Canevesi[c], Júlio Takehiro Marumo[a]

[a] Instituto de Pesquisas Energéticas e Nucleares, Av. Prof. Lineu Prestes, 2242 – Cidade Universitária, São Paulo, SP, 05508-000, Brazil
[b] Itatijuca Biotech, Av. Prof. Lineu Prestes, 2242, USP/IPEN/CIETEC, Sala 107 – Cidade Universitária, São Paulo, SP, 05508-000, Brazil
[c] Universidade Estadual Do Oeste Do Paraná, Rua da Faculdade 645 - Jardim La Salle, Toledo, PR, 85903-000, Brazil

A B S T R A C T

Biosorption-based technologies have been proposed for the removal of radionuclides from radioactive liquid waste containing organic compounds. Nevertheless, pytoremediation potential of uranium (U) by nonliving aquatic macrophytes *Lemna* sp. and *Pistia stratiotes* has not been previously addressed. In this study, uranium biosorption capacity by *Pistia stratiotes* and *Lemna* sp. was evaluated by equilibrium and kinetics experiments. The biomasses were added to synthetic and real waste solutions. The assays were tested in polypropylene vials containing 10 mL of uranium nitrate solution and 0.20 g of biomass. Solutions ranging from 0.25 to 84.03 mmol l^{-1} were employed for the assessment of uranium concentration in each macrophyte. The equilibrium time was 1 h for both macrophytes. *Lemna* sp. achieved the highest sorption capacity with the use of the synthetic solution, which was 0.68 mmol g^{-1} for the macrophyte. Since *Lemna* sp. exhibit a much higher adsorption capacity, only this biomass was exposed to the actual waste solution, being able to adsorb 9.24×10^{-3} mmol g^{-1} U (total). The results show that these materials are potentially applicable to the treatment of liquid radioactive waste.

1. Introduction

The techniques most used in the nuclear industry to treat radioactive liquid waste (RLW) are incineration, evaporation, and chemical precipitation. All these techniques have advantages and disadvantages, but in general, are expensive and unfeasible for the low volume of radioactive liquid waste. Consequently, alternative processes have been studied to treat these solutions.

In the last decades, biosorption has been studied as an alternative in removing radionuclides in Intermediate-Level Long-Lived Waste (ILW-LL), since this process has low cost, do not require high technology, and have a wide range of materials to be used (Volesky, 2003). Many studies reported the biosorption ability of different biomasses to remove radionuclides from solutions, such as banana peels (Oyewo et al., 2016), coconut fiber (Ferreira et al., 2018), *Padina* sp. algae (Khani, 2011) and *Catenellarepens*, red algae (Bhat et al., 2008), among others.

A good biosorbent has some characteristics, such as efficient and rapid sorption/desorption of the metal, high selectivity, reusability, and easy separation from solutions (Volesky, 1987). Macrophytes have all these characteristics. They are aquatic species that have been demonstrated as a material with a capacity of adsorbing heavy metals in effluents (Khosravi et al., 2005) and the potential to remove radionuclides from liquid ILW-LL. They inhabit diverse environments ranging from lakes, waterfalls, swamps, dams, basins and even salty environments such as coral reefs. The same species of macrophytes are found inhabiting various environments and their versatility is such that they resist long periods of drought. This demonstrates that these materials can be easily found and extracted from nature because of their versatility and adaptation to the most diverse climates and conditions. Moreover, these materials can be cultivated intensively and with low cost; coupled with their high capacity in the retention of heavy metal ions. In this context, macrophytes can become an efficient and attractive means of treatment of radioactive waste.

Pistia stratiotes L. is a floating aquatic macrophyte that proliferates in tropical aquatic ecosystems. This plant species is found on the north, northern, center-west, south, and southeast regions of Brazil and it develops on all kinds of freshwater: pure, polluted, muddy or stagnant (Forzaa, 2010; Cancian et al., 2009). *Lemna* spp. are also floating aquatic macrophytes that inhabit the most diverse places such as rivers, lakes and even cities, with a vegetative development in which one plant gives origin to another, facilitating their multiplication. The amount of this plant can double in up to a week. *Lemna* sp. has been used to feed animals such as cattle, poultry, and pigs with favorable results (Skillicorn et al., 1993). According to Tavares (2004), the introduction of *Lemna* sp. in tilapia feeding showed satisfactory results in relation to their weight gain, indicating that they can be used as a food source.

Both plants can be useful for treating radioactive liquid wastes because they are easily acquired due to their natural abundance and have a high growth rate that easily enables sustainable use. In literature, there are several studies on the use of aquatic macrophytes in the

* Corresponding author.
E-mail address: lgoulart@usp.br (L.G. de Araujo).

https://doi.org/10.1016/j.jenvrad.2019.03.019
Received 7 February 2019; Received in revised form 15 March 2019; Accepted 16 March 2019
Available online 27 March 2019
0265-931X/

removal of heavy metals. These studies demonstrated high efficiency in the removal of metal(loid)s ions, such as gold (Umali et al., 2006); cadmium (Maine et al., 2001); uranium and arsenic (Mkandawire et al., 2004; Mkandawire, 2005); chromium (III) and chromium (IV) (Elangovan et al., 2008), and nickel (Kara 2012).

According to Sheppard et al. (2005), risks of radionuclides are usually evaluated by the total radiological dose rate to target organisms. For uranium, the isotopic composition is crucial for determining if the risk is greater from a chemical or radiological point of view. Sheppard et al. (2005) found that uranium intake may interfere in growth and development rates of living organisms, as well as other issues, such as renal damage.

Different investigations are reported in the literature, in which the biosorption process was applied to remove uranium in aqueous matrices. Sar and D'Souza (2001) studied uranium uptake of live and lyophilized *Pseudomonas* cells. Uranium binding reached > 90% sorption efficiency in only 10 min of contact and the equilibrium was accomplished after 60 min. It is worth observing that lyophilized *Pseudomonas* exhibited a higher metal loading compared to the living organisms, 541 versus 410 mg g^{-1}, respectively. Wang et al. (2010) employed *Rhizopus arrihizus* to remove uranium. The results indicated that *R. arrihizus* is able to grow in the presence of high uranium concentration (200 mg L^{-1}) and presented a maximum biosorption capacity of 112 mg g^{-1} in optimum conditions. A recent review of the literature on this topic (Gök et al., 2017) found that raw and modified brown macroalgae *Cystoseria* sp. are able to remove uranium from aqueous solutions. The modified biomass presented higher uranium uptake values. According to their biosorption model, the maximum biosorption capacity of this biomass is 468.01 mg g^{-1}. Bağda et al. (2017) investigated the biosorption of uranium by the green algae *Cladophora hutchinsiae*. Under optimal batch conditions (pH: 5, biosorbent concentration: 12 g L^{-1}, contact time: 60 min, temperature: 20 °C), the biosorption capacity was 152 mg g^{-1}. More recent evidence (Bağda et al., 2018) highlights that the macrofungus *Russula sanguinea* is capable of removing 174 mg g^{-1} of uranium at pH 5 and 20 °C. The cycling test indicated that this biosorbent presents a good sorption/desorption performance. The biosorption processes have demonstrated similar sorption capacities when compared to other sorbents. For instance, Saleh et al. (2017) evaluated polyethyleneimine modified activated carbon/Fe to remove uranium from aqueous solution. The maximum adsorption capacity achieved was 115 mg g^{-1} under optimized conditions. This value is close to those measured by the references cited herein.

The objective of this work was to evaluate the biosorption capacity of aquatic macrophytes *Pistia stratiotes* and *Lemna* sp. when exposed to different concentrations of uranium in solution. As far as we know, the aquatic macrophytes employed in this work have not been previously investigated regarding their ability to reduce uranium in synthetic solutions, as well as *Lemna* sp.'s ability to reduce this radionuclide in real radioactive liquid waste. Furthermore, sorption kinetic models have not been proposed for uranium biosorption using these biomaterials.

2. Materials and methods

The methodology adopted in this study was divided into two steps: i) preparation and characterization of the biomasses and ii) biosorption assays.

2.1. Biomass

The macrophytes *Pistia stratiotes* and *Lemna* sp. were provided by Universidade Estadual do Oeste do Paraná (UNIOESTE). Both biomasses were washed and dried (Fanem, Brazil) to constant mass at 60 °C for 24 h, triturated (Arno, Brazil), sieved (Telastem, Brazil), and separated to obtain particle sizes between 0.297 mm and 0.125 mm. These particle sizes were chosen in view of the good results obtained by Ferreira et al. (2018). Following this, the biomasses were sterilized by ultraviolet (UV) radiation (Hexiclean, China) for 30 min to prevent deterioration by fungal or bacterial proliferation, and finally stored for later use.

2.2. Preparation of synthetic solution

The uranium solutions were prepared by dissolving uranium nitrate (Merck, Brazil) in distillate water with previously adjusted pH. The pH adjustments were made adding nitric acid (Merck, Brazil) and sodium hydroxide (Merck, Brazil) into solution. The solution pH was fixed at 4 because it is a common pH to be found in the radioactive wastes at the Radioactive Waste Management of IPEN-CNEN/SP. There are also evidence in the literature that this pH favors uranium biosorption, since at this pH uranium uptake was higher. Some studies indicate that this occurs due to the speciation of uranium in water (Yang and Volesky, 1999). Exploratory tests were made with pH 2.17, which is the value of the real liquid waste. As the results were unsatisfactory, tests were made with pH 4 (based on the literature) resulting in higher sorption capacity.

2.3. Physical characterization

The parameters evaluated in the physical characterization of biomass were the morphological characteristics of macrophytes, real and apparent density, specific surface area, and analysis of atomic absorption spectroscopy (AAS) in the infrared region with Fourier transform.

The morphological characteristics of the crude biomasses were analyzed using scanning electron microscopy (SEM) by microscope (Philips, Netherlands). The macrophytes were oven dried for 24 h at 80 °C, and thereafter the samples were coated with a thin, electric conductive gold film. The real biomass density was obtained using the helium gas pycnometry technique (Vilar et al., 2007) (Micromeritcs, USA). According to Lima and Marshall (2005), the apparent density of the macrophytes was determined by means of the relationship between mass and volume. The specific surface area was determined according to the Brunauer, Emmet, and Teller (B.E.T) method (Micromeritcs, USA) reported by (Ren et al., 2009). This method is based on the nitrogen adsorption–desorption isotherms at 77 K (Brunauer et al., 1938; Danish et al., 2012). Fourier Transform Infrared Spectroscopy (FTIR) identified the functional groups present in the macrophyte structure. Analyzes were performed on a spectrometer (Perkin Elmer, USA) with an ATR germanium crystal. The spectrum was analyzed in the region of 600–4000 cm^{-1}.

2.4. Biosorption experiments

The kinetics and equilibrium biosorption experiments were conducted in a batch system. All experiments were performed in triplicate for each of the macrophytes. Exact 0.2 g of biomass was put into contact with 10 mL of solution. The kinetics biosorption studies were carried out with synthetic solutions with an initial uranium concentration of 0.63 mmol L^{-1}. The equilibrium experiments were performed with synthetic solutions at different initial concentration ranged from 0.25 to 84 mmol L^{-1}. Assays were also made with real liquid radioactive waste (LRW), which presents a uranium concentration of 0.25 mmol L^{-1}, but only with the use of the *Lemna* sp. as adsorbent material. The other experimental conditions were the same for the kinetic and equilibrium experiments.

The system was incubated in an orbital shaker (Biothec, Brazil) at controlled stirring speed (130 rpm) and at room temperature (≈ 21 °C). In the equilibrium experiments, the samples were shaken long enough to ensure the adsorption equilibrium was reached. The contact times were 5, 30, 60, 120 and 240 min and the experiments were performed in triplicate for each of the macrophytes. Subsequently, the biomasses were separated by filtration with paper filters (slow filtration for fine

precipitates with an ash content of 0.00012 g) (Millipore, USA). Furthermore, a new filtration was carried out with a vacuum system (0.1 μm polypropylene filter) (Millipore, USA) to avoid the presence of any biomass residues in the remaining solution that could interfere with the results.

2.5. Determination of U by ICP-OES

The solution concentration was determined by inductively coupled plasma optical emission spectroscopy (ICP-OES), model Optima 7000DV (Perkin Elmer, USA). Calibration solutions were prepared by dilution of certified uranium solution (Johnson Matthey Company, UK). The wavelength (λ) used in the determination of uranium was 424.167 nm, and the result is expressed as the average of triplicate measurements.

2.6. Mathematical adsorption modeling

2.6.1. Data evaluation

The uptake of uranium by the biomass in a bath adsorption experiment was determined using the following equation Eq. (1):

$$q = (C_o - C)\frac{V}{m} \quad (1)$$

where q is the uptake of uranium (mmol g^{-1}), Co is the initial uranium concentration in solution (mmol L^{-1}), C is the equilibrium concentration in solution (mmol L^{-1}), V is the volume of solution (L), and m is the mass of biosorbent (g).

2.6.2. Biosorption isotherms

The biosorption isotherm represents the equilibrium existent between the biomass and the solution at a given condition. It reveals how biosorption behaves as the metal concentration in solution varies.

The adsorption equilibrium is graphically represented by adsorption isotherms that express the relationship between the concentration of ions retained in the biosorbent material and the amount remaining in solution. The isotherms are based on mathematical models and the parameters of adsorption isotherms models are obtained from the data gathered experimentally. Their physicochemical parameters, together with the assumptions of the models, provide insight into the adsorption mechanism as well as the degree of affinity of the adsorbents (Foo and Hameed, 2010).

In this context, in order to adequately describe the adsorption equilibrium data, one should first choose an equation that describes the data collected with accuracy and, secondly, regression methods must be applied to find the optimal parameters (Hinz, 2001). Over the years, various models have been formulated, being the most used the Langmuir and Freundlich models because of their easy application and interpretation.

This paper investigates several adsorption isotherms models, namely: Langmuir, Freundlich, Sips, Redlich-Peterson, Two-Sites Langmuir, and Radke-Prausnitz.

These models were used to describe the data in the range of concentrations studied and are listed in Table 1 with their respective equations.where in Langmuir model q_{eq} is the quantity per unit mass of the species (metal) adsorbed at equilibrium (mmol g^{-1}), Q_o is the maximum adsorption capacity (mmol g^{-1}), k_L is the Langmuir constant related to adsorption energy (L $mmol^{-1}$) and C_e is the concentration of adsorbed adsorbate when the system is at equilibrium (mmol L^{-1}). In the Freundlich model, K_f is a constant related to adsorption capacity (L $mmol^{-1}$), n is a constant that represents the sorption intensity and the distribution of the active sites; when $0 < {}^{1}/_{n} \leq 1$, there is favorable adsorption of the chemical species in the adsorbent and when ${}^{1}/_{n} > 1$ it is considered unfavorable adsorption of the chemical species in the adsorbent. In Sips model, k_s is the constant related to adsorption energy (L $mmol^{-1}$), a_s is the Sips constant (L $mmol^{-1}$) and β_s indicates the heterogeneity of the biosorbent; Note that if $\beta_s = 1$, the model reduces to Langmuir. In the Redlich–Peterson model, K_{R_p} is the first constant of the isotherm R-P (mol^{-1}), a_{R_p} is the second R-P isotherm constant (L $mmol^{-1}$), g is an exponent whose value comprises between 0 and 1. Note that if $g = 1$, the model reduces to the Langmuir isotherm and if $g = 0$, it reduces to a Freundlich isotherm. In Two-Site Langmuir model, Q_1 and Q_2 are the adsorption capacities (mmol g^{-1}) and the maximum capacity is the sum of $Q_1 + Q_2$, b_1 and b_2 are the affinity coefficients of sites 1 and 2 respectively (L $mmol^{-1}$). Finally, in Radke-Prausnitz model q_{max} is the maximum adsorption capacity (mmol g^{-1}), K_{RP} is the Radke-Prausnitz constant related to adsorption energy (L $mmol^{-1}$) and n_{RP} is the dimensionless exponent of Radke-Prausnitz.

Table 1
Adsorption isotherm models used to describe data.

Model	Equation	nº	Reference
Langmuir	$q_{eq} = \frac{Q_0 k_L C_e}{1 + k_L C_e}$	(2)	Foo and Hameed (2010)
Freundlich	$q_{eq} = k_f C_e^{\frac{1}{n}}$	(3)	Foo and Hameed (2010)
Sips	$q_{eq} = \frac{k_s C_e^{\beta_s}}{1 + a_s C_e^{\beta_s}}$	(4)	Foo and Hameed (2010)
Redlich–Peterson	$q_{eq} = \frac{K_{RP} C_e}{1 + a_{RP} C_e^{g}}$	(5)	Foo and Hameed (2010)
Two-Site Langmuir	$q_{eq} = \left(\frac{Q_1 b_1 C_e}{1 + b_1 C_e} + \frac{Q_2 b_2 C_e}{1 + b_2 C_e}\right)$	(6)	Hinz (2001)
Radke-Prausnitz	$q_{eq} = \frac{q_{max} K_{RP} C_e}{(1 + K_{RP} C_e)^{\frac{1}{n_{RP}}}}$	(7)	Foo and Hameed (2010)

These adsorption isotherm models were utilized to describe the equilibrium between the biomass and the solution. However, these models contain several theoretical assumptions that cannot be fully accredited to biosorption systems because of the complex chemical structure of biological materials (Gadd, 2009). They are useful however to quantitatively describe the sorption data in the range of concentrations studied herein. In addition, qualitative experiments can be conducted to reveal some of the mechanisms of the biosorption system and to prove or reject the theoretical assumptions.

2.6.3. Sorption kinetics

Determining the kinetics of biosorption is fundamental to evaluate the efficiency of the removal of metals by macrophytes. Sorption kinetics describes the adsorption rate of the solute, determining the rate and equilibrium time at which sorption occurs.

Several independent processes can control sorption kinetics, such as:

- External mass transfer process including mass diffusion of the absorbance in solution, and diffusion film across the boundary of the biosorbent.
- Intra-particle diffusion of the adsorbate from the inner surface
- Chemical interactions involving reactions between the active sites in the biosorbent and adsorbate (Auta and Hameed, 2013).

Lagergren's pseudo-first-order and Pseudo-Second Order models were used to analyze the kinetics of uranium biosorption by macrophytes *Lemna* sp. and *Pistia stratiotes*.

2.6.4. Estimation of parameters

Recently, errors inherent have been pointed out in the use of linear methods to estimate isotherm parameters (El-Khaiary and Malash, 2011; Kumar and Sivanesan, 2007; Foo and Hameed, 2010). For this reason, the parameters of the isotherm and kinetic models were estimated by applying the Nelder-Mead Simplex optimization method to the experimental data. The objective function used in this method is given by Eq. (8), where q^{EXP} and q^{CAL} are, respectively, the experimentally and the calculated amounts of uranium uptake per mass of

biomass and n is the number of experimental data.

$$F_{obj} = \sum_{j=1}^{n} (q^{EXP} - q^{CAL})^2 \quad (8)$$

As usual, the correlation coefficient (R^2) was used to measure how well experimental data fit the isotherm models. Also, the equilibrium models fit were evaluated by the corrected Akaike information criterion (AIC) according to the following equation:

$$AIC = n\ ln\left(\frac{\sum_{j=1}^{n}\left(q^{EXP} - q^{CAL}\right)^2}{n}\right) + 2(p+1) \quad (9)$$

where p is the number of adjustable parameters.

3. Results and discussion

3.1. Physical characterization

Morphological analyzes of biomasses *Pistia stratiotes* and *Lemna* sp. performed by scanning electron microscopy are presented in Fig. (1) and (2).

Fig. (1) and (2) indicate that both macrophytes have irregular structures. *Lemna* sp. biomass presents a more uniform and compact surface compared to *Pistia stratiotes*. Information about the porosity of the biomasses was not obtained by scanning electron microscopy.

Energy dispersive X-ray spectrometry (EDS) analyses of the macrophytes, as seen in Table 2, revealed a distinct chemical composition between them. For instance, *Pistia stratiotes* and *Lemna* sp. indicated a high percentage of calcium and potassium, respectively.

Pistia stratiotes presents a high percentage of calcium (Ca) that has the stabilizing function of the cell wall in the cell membrane system and in the middle lamella connecting the pectin radicals (Volk et al., 2004). Potassium (K) is present in a higher percentage in the macrophyte *Lemna* sp., being an enzymatic activator in the ATP synthesis of carbohydrates, in respiration and protein synthesis. Plants with potassium deficiency demonstrate lower protein synthesis and accumulation of soluble nitrogen compounds, such as amino acids, nitrates, and amides (Borgatto et al., 2002).

3.2. Real density, apparent density, and surface area

As for the densities, *Pistia stratiotes* (real density: 1.600 ± 0.001 g cm^3; apparent density: 0.34 ± 0.02 g cm^3) and *Lemna* sp. (real density: 1.690 ± 0.001 g cm^3; apparent density: 0.30 ± 0.01 g cm^3), it can be stated that the values obtained for both macrophytes are very close, although the microscopic analysis shows that they have different appearances. The specific surface area was measured and *Pistia stratiotes* indicated a larger specific surface area (13.80 ± 0.70 m^2 g^{-1}), compared to *Lemna* sp. (6.60 ± 0.70 m^2 g^{-1}). It is worth mentioning that a larger surface area represents a higher adsorption intensity since this process is a surface phenomenon.

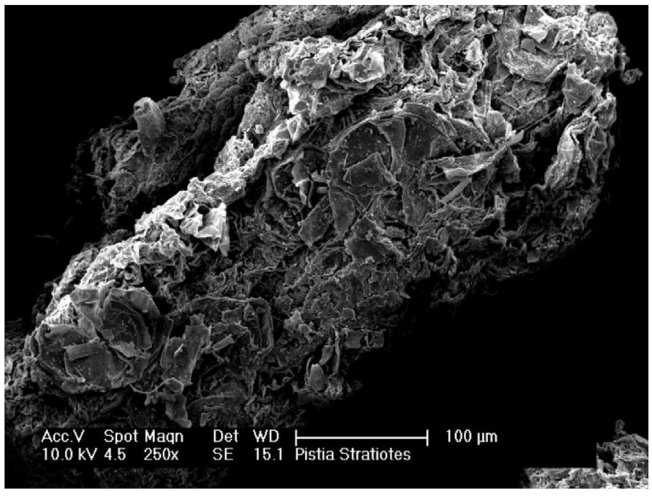

Fig. 1. Micrographs of raw biomass *Pistia stratiotes*.

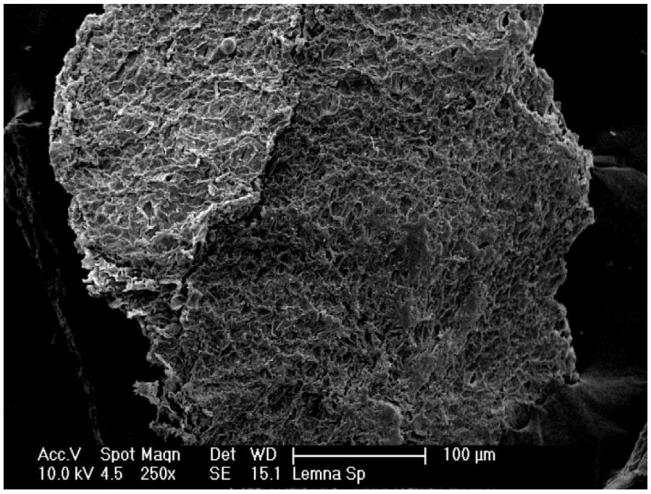

Fig. 2. Micrographs of raw biomass *Lemna* sp.

Table 2
Percentage result of EDS analysis of macrophytes.

Element	Biomasses	
	Pistia stratiotes	*Lemna* sp.
Na	1.40	0.90
Mg	3.70	1.60
Al	–	–
Si	–	2.00
P	–	1.80
S	0.40	2.00
Cl	4.30	10.80
K	19.60	43.90
Ca	52.50	28.80
Fe	18.10	6.20
Mn	–	2.00

3.3. Fourier transform infrared spectroscopy (FTIR)

Functional groups identified by the transmittance spectra obtained by FTIR of biomasses before biosorption process are presented in Table 3. *Pistia stratiotes* and *Lemna* sp. spectra are observed in Fig. 3 (a)

Table 3
Identification of the functional groups present in *Pistia stratiotes* and *Lemna* sp.

Biomass	Wave number (cm^{-1})	Functional group
Pistia stratiotes	3323	-O-H, -N-H
	2917	-CH
	2851	-CH
	1614	-N-H
	1030	-C-O
	780	-C-C
Lemna sp	3281	-O-H, -N-H
	2919	-C-H
	1626	-N-H
	1030	-C-O

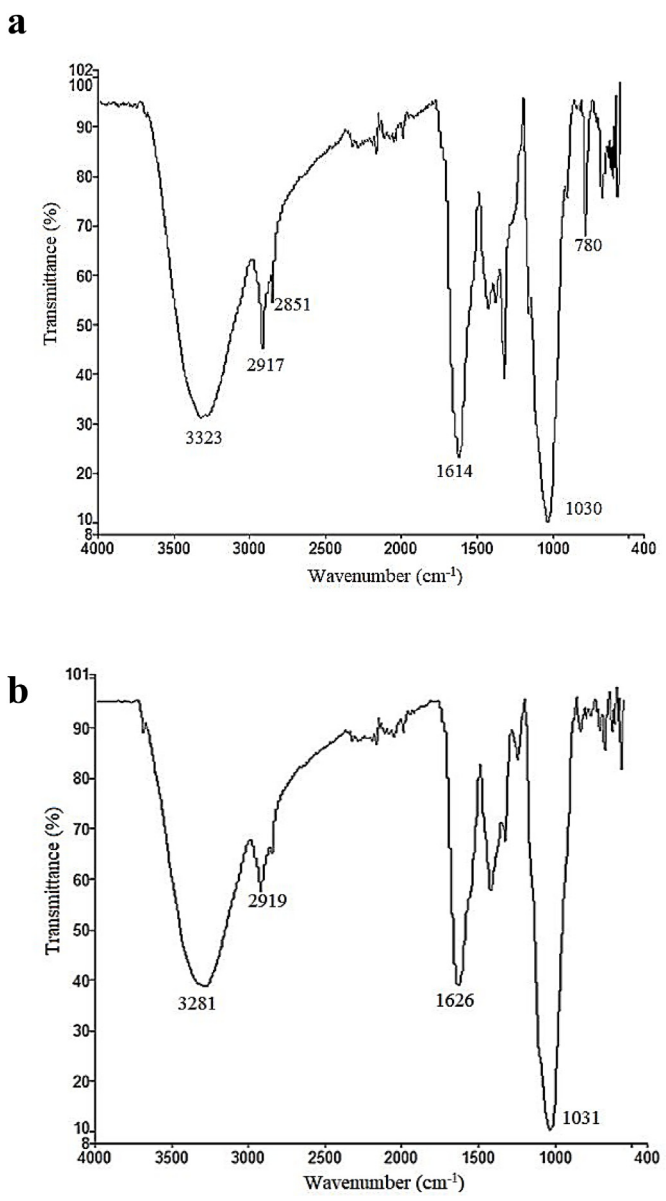

Fig. 3. FTIR spectra of biomass (a) *Pistia stratiotes*; (b) *Lemna* sp.

and (b), respectively.

Figs. 3 and 4 suggest the presence of the functional groups listed in Table 3. The wide absorption band located at 3323 cm^{-1} for *Pistia stratiotes* and at 3281 cm^{-1} for *Lemna* sp. shows overlap of OH and NH, indicating the presence of two groups of free hydroxyls on surface and water (Sari et al., 2008; Uluozlu et al., 2008; Tuzen et al., 2008; Salman et al., 2010). The bands 2919 cm^{-1} and 2850 cm^{-1} located in the *Pistia stratiotes* spectrum and the 2919 cm^{-1} and 2920 cm^{-1} bands in the *Lemna* sp. spectrum correspond to the CH stretching (Sari et al., 2008; Sari and Tuzen 2008, 2009; Uluozlu et al., 2008; Pavia et al., 2008, Tuzen et al., 2008). The bands in 1614 cm^{-1}, 1618 cm^{-1}, 1626 cm^{-1} and 1624 cm^{-1} are characteristics of the folding presence of the amine group (NH), also indicating the presence of water (Salman et al., 2010). The stretching vibrations of CO with single bonds are present in the 1030 cm^{-1} band for both studied macrophytes (Sari et al., 2008; Sari and Tuzen, 2008; Uluozlu et al., 2008, Tuzen et al., 2008). The spectra below the 600 cm^{-1} region were considered as noise.

According to Fourest and Volesky (1996), the functional groups responsible for biosorption in aquatic macrophytes are amines, carboxylates, carbonyls, hydroxyls, sulfonates, and thiols. The amine and

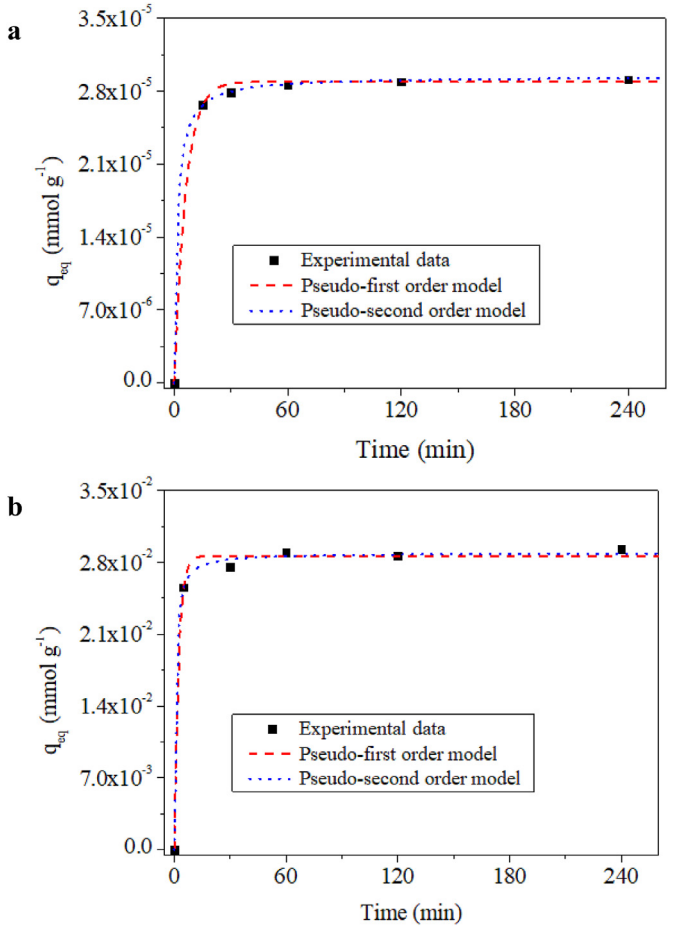

Fig. 4. Experimental data and model biosorption kinetics of uranium into macrophytes. (a) *Pistia stratiotes;* (b) *Lemna* sp.

Table 4
Parameters of kinetics calculated for the biomasses adopted.

Model		*Pistia stratiotes*	*Lemna* sp.
Pseudo- first order	^{qeq} (mmol g^{-1})	2.89×10^{-2}	2.90×10^{-2}
	K_1 (min^{-1})	0.17	0.45
	$_R2$	1.00	1.00
Pseudo-second order	^{qeq} (mmol g^{-1})	2.81×10^{-2}	2.89×10^{-2}
	K_2 (g $mmol^{-1}$ min^{-1})	21.75	51.51
	$_R2$	1.00	1.00

carboxyl groups were previously identified in the literature as responsible for uranium biosorption by the macrophyte *Eichhornia crassipes* (Yi et al., 2016).

The identified hydroxyl OH that can be attributed to the presence of alcohols and carboxylic groups, and the amine group NH_2 are present in both macrophytes, thus being able to participate directly in the biosorption process.

3.4. Biosorption assays

3.4.1. Biosorption kinetics

The results of uranium biosorption versus time for the macrophytes *Pistia stratiotes* and *Lemna* sp. are presented in Fig. 4.

The results of the biosorption experiments show that the uranium concentration in the biomass increased as a function of time until the equilibrium was reached. This behavior is expected since uranium accumulates in the biomass at the adsorption sites until the dynamic

Table 5
Comparison of uranium uptake by employing different biomasses.

Biomass	Type of solution	Uranium biosorption capacity (mmol g^{-1})	Reference
Pistia stratiotes	Synthetic	2.86×10^{-2}	This work
Lemna sp.	Synthetic	6.81×10^{-1}	This work
	Real radioactive waste	9.24×10^{-3}	This work
Raw coconut fiber	Real radioactive waste	2.77×10^{-3}	Ferreira et al. (2018)
Activated coconut fiber	Real radioactive waste	7.65×10^{-3}	Ferreira et al. (2018)
Eichhornia crassipes	Synthetic	6.00×10^{-1}	Yi et al. (2016)
Lyophilized *Pseudomonas* strain	Synthetic	2.27×10^{-3}	Sar and D'Souza (2001)
Live *Pseudomonas* strain	Synthetic	1.72×10^{-3}	Sar and D'Souza (2001)
Potamogeton pectinatus L.	Synthetic	6.55×10^{-3}	Pratas et al. (2014)
Cladophora hutchinsiae	Synthetic	6.38×10^{-4}	Bağda et al. (2017)
Russula sanguinea	Synthetic	7.32×10^{-4}	Bağda et al. (2018)

Table 6
Parameters calculated by adsorption isotherm models regarding uranium biosorption onto *Pistia stratiotes* and *Lemna* sp. and the correlation coefficients obtained for each model.

Biomass	Model	Parameters					
Pistia stratiotes	Langmuir	Q (mmol g^{-1})	K_L (L $mmol^{-1}$)			R^2	AIC
		3.67×10^{-2}	26.50			0.78	−174.3
	Freundlich	K_f (L $mmol^{-1}$)	1/n			R^2	AIC
		2.52×10^{-6}	0.49			0.85	−177.2
	Sips	K_s (L $mmol^{-1}$)	a_s (L $mmol^{-1}$)	β_s		R^2	AIC
		2.52×10^{-6}	3.03×10^{-10}	4.86×10^{-1}		0.86	−175.2
	Redlich Peterson	K_{RP} (mol^{-1})	a_{RP} (L $mmol^{-1}$)	β		R^2	AIC
		0.69	5.15	1.07×10^{-1}		0.86	−175.2
	Two-Site Langmuir	Q_1 (mmol g^{-1})	Q_2 (mmol g^{-1})	b_1 (L $mmol^{-1}$)	b_2 (L $mmol^{-1}$)	R^2	AIC
		1.84×10^{-2}	2.21×10^{-8}	17.4	25.5	0.90	−170.1
	Radke-Prausnitz	q_{max} (mmol g^{-1})	K_{RP} (L $mmol^{-1}$)	n_{RP}		R^2	AIC
		2.79×10^{-2}	36.10	8.56×10^{-1}		0.80	−172.7
Lemna sp.	Langmuir	Q (mmol g^{-1})	K_L (L $mmol^{-1}$)			R^2	AIC
		7.37×10^{-1}	0.98			0.98	−197.5
	Freundlich	K_f (L $mmol^{-1}$)	1/n			R^2	AIC
		2.18	0.30			0.91	−181.1
	Sips	K_s (L $mmol^{-1}$)	a_s (L $mmol^{-1}$)	β_s		R^2	AIC
		0.43	0.57	9.32×10^{-1}		0.98	−195.8
	Redlich Peterson	K_{RP} (mol^{-1})	a_{RP} (L $mmol^{-1}$)	β		R^2	AIC
		0.35	1.63×10^{2}	7.01×10^{-1}		0.91	−179.2
	Two-Site Langmuir	Q_1 (mmol g^{-1})	Q_2 (mmol g^{-1})	b_1 (L $mmol^{-1}$)	b_2 (L $mmol^{-1}$)	R^2	AIC
		0.28	0.48	0.32	1.57	0.98	−194.1
	Radke-Prausnitz	q_{max} (mmol g^{-1})	K_{RP} (L $mmol^{-1}$)	n_{RP}		R^2	AIC
		0.19	11.60	7.68×10^{-1}		0.95	−184.3

Parameters predicted by the adsorption isotherm models regarding uranium biosorption onto *Pistia stratiotes* and *Lemna* sp. and the correlation coefficients obtained for each model.

equilibrium occurs. The equilibrium is reached as the desorption rate approaches the rate of biosorption (Foo and Hameed, 2010). The equilibrium time was reached after 60 min for both macrophytes.

The models of Pseudo-first order and Pseudo-second order were selected by using the curves of experimental versus calculated data. These models were also evaluated for the uranium biosorption kinetics. The values of the parameters obtained for each kinetic model and their graphical representations are outlined in Table 4 and Fig. 4, respectively.

According to the correlation coefficient R^2 (1.00), both pseudo-first and pseudo-second-order models fitted to the experimental data in the sorption behavior of both macrophytes.

3.4.2. Biosorption capacity

The highest values of sorption capacity of uranium were observed with *Lemna* sp. ($6.81 \times 10^{-1} \pm 7.56 \times 10^{-3}$ mmol g^{-1}) for the synthetic solution. *Pistia stratiotes* revealed a much lower sorption capacity, which was $2.86 \times 10^{-2} \pm 2.52 \times 10^{-4}$ mmol g^{-1}. No studies were found in the literature that could be used to directly compare the results obtained. There are, however, many works on bioaccumulation and phytoremediation related to other macrophytes and metals, but scarce for uranium. For example, *Eichhornia crassipes* macrophyte was studied by (Yi et al., 2016) for uranium biosorption in simulated radioactive waste solutions. The uranium biosorption capacity was 6.00×10^{-1} mmol g^{-1}, slightly lower than the results obtained in this work.

The behavior of the macrophyte *Lemna aequinoctialis* was studied in the presence of uranium and copper, but with a different purpose, which was to evaluate the toxicity of these metals in the plant growth (Charles et al., 2006). The author verified that this macrophyte, by means of the bioaccumulation, retains these metals influencing negatively in its growth.

The macrophytes *Callitriche stagnalis Scop*, *Potamogeton natans* L., and *Potamogeton pectinatus* L. were evaluated by Pratas et al. (2014) for bioaccumulation of uranium. The best results of sorption capacity obtained by authors were using the macrophyte *Potamogeton pectinatus* L. presented uranium sorption capacity of 6.55×10^{-3} mmol g^{-1}, much lower than those obtained in this work.

Since *Lemna* sp. indicated a much higher biosorption capacity of uranium uptake, only this macrophyte was evaluated with real LRW. *Lemna* sp. sorption capacity with real radioactive waste was $9.24 \times 10^{-3} \pm 8.40 \times 10^{-4}$ mmol g^{-1}. This value was slightly higher than those reported by Ferreira et al. (2018). In this work, biomasses of raw coconut fiber and activated coconut fiber presented a uranium

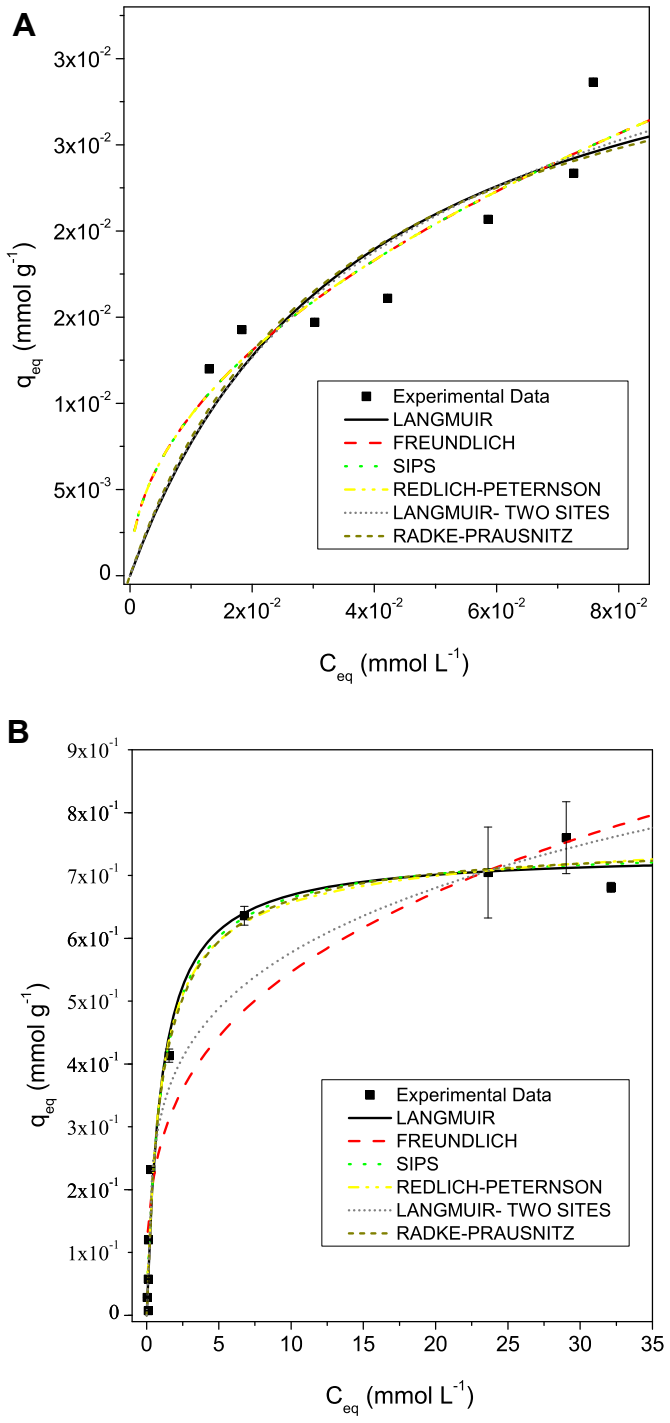

Fig. 5. Experimental equilibrium isotherm data and calculated by isotherms models. (a) *Pistia stratiotes*; (b) *Lemna* sp.

biosorption capacity of $2.77 \times 10^{-3} \pm 4.20 \times 10^{-4}$ mmol g^{-1} and $7.65 \times 10^{-3} \pm 1.68 \times 10^{-4}$ mmol g^{-1}, respectively. These values were also obtained by employing real radioactive waste with uranium concentration of 0.25 mmol L^{-1}. Table 5 compares the results obtained by our work, with several collected in literature.

Comparing the values obtained with the uranium solution and the real waste, higher sorption capacities were observed in the uranium solution, which could be explained by the experimental conditions adopted. In this case, single element solutions (uranium) were utilized with only one element (uranium) and prepared with an adequate pH for the biosorption. The real radioactive waste, in turn, consists of a solution with organic compounds, multi-elementary (uranium, americium, and cesium) and pH 2.17. In addition to the low pH, different from the range stipulated as optimal pH in uranium biosorption (Panias and Krestou, 2015; Michalak et al., 2013), the competition of the elements by the adsorption sites of the biomass must also be considered.

Among the biomasses tested, *Lemna* sp. presented the highest removal capacity in a shorter time, probably because of its larger specific relative area, since the adsorption sites would be more available.

Table 6 highlights the parameters of the isotherms obtained for the macrophytes *Lemna* sp. and *Pistia stratiotes*. Afterward, Fig. 5 depicts the experimental versus the calculated data by the isotherm models.

According to the correlation coefficient R^2 (0.95) for the macrophyte *Pistia stratiotes*, the Redlich-Peterson isotherm model was the most adequate as regards the experimental data. This model is a hybrid isotherm that combines the characteristics of the Langmuir and Freundlich models, representing the adsorption equilibrium over a wide concentration range. The exponent β is between 0 and 1 and indicates a larger trend for one of these models. The closer to 1 the greater the trend for Langmuir and the closer to zero for Freundlich (Zelentsov et al., 2012). For *Pistia stratiotes*, the value of β was equal to 1, indicating there is a greater tendency for the Langmuir model, which takes adsorption in monolayer with fixed numbers of adsorption sites. These sites are uniform and the reaction occurs between a single molecule and a single active site, with no interaction between the adsorbed species.

In the case of the *Lemna* sp., all the models fit the results, but Langmuir's showed the best fit. The constant β of the Redlich-Peterson isotherm model demonstrates it, with a value closer to 1. The value of n_{RP} parameter of Radke-Prausnitz isotherm also reinforces this information. The maximum experimental capacity was very close to the theoretical ones obtained in the three models: Langmuir, Langmuir two sites, and Radke-Prausnitz. The process then assumes a biosorption with fixed numbers of adsorption sites, where all sites are uniform and accommodate only a single molecule, and there is no interaction between adsorbed species (Foo and Hameed, 2010).

4. Conclusions

The biosorption capacity of the aquatic macrophytes of the species *Pistia stratiotes* and *Lemna* sp. was evaluated under different concentrations of uranium in synthetic solution and real radioactive waste. Only *Lemna* sp. was studied in uranium sorption in real radioactive waste, because it presented a maximum sorption capacity (experimentally: 6.81×10^{-1} mmol g^{-1}; calculated: 7.37×10^{-1} mmol g^{-1}) far superior to *Pistia stratiotes* (experimentally: 2.86×10^{-2} mmol g^{-1}; calculated: 3.67×10^{-2} mmol g^{-1}) in the synthetic solutions. *Lemna* sp. sorption capacity with real radioactive waste was much lower: 9.24×10^{-3} mmol g^{-1}. The complex nature of the radioactive liquid may have interfered in the sorption process negatively. These two macrophytes present distinct appearance and surface areas, but they have the same functional groups acting directly in the biosorption process. Optimum contact time for uranium removal was experimentally determined as 60 min for both macrophytes.

Isotherm models were efficient in the understanding of the uranium biosorption process by the studied macrophytes. Redlich-Peterson and Langmuir were the models that best fit the experimental data for *Pistia stratiotes* and for *Lemna* sp., respectively.

The findings of this study indicate that macrophytes are biosorbents that are easy to handle, stable and have the potential to be applied in the treatment of radioactive waste.

Finally, further work is required to evaluate *Lemna* sp. behavior under higher uranium concentrations. Moreover, the utilization of *Lemna* sp. in treating multi-metals solutions is crucial, since this biomaterial could be utilized in wastes that are more complex. An important matter to resolve for future studies is the immobilization of these biomasses in cement. The evaluation of other macrophytes seems

also interesting and necessary, considering the differences found in uranium uptake by the two macrophytes herein evaluated.

Acknowledgments

This study was supported by the Nuclear and Energy Research Institute, the Brazilian National Nuclear Energy Commission and the Brazilian National Council for Scientific and Technological Development.

References

Auta, M., Hameed, B.H., 2013. Acid modified local clay beads as effective low-cost adsorbent for dynamic adsorption of methylene blue. J. Ind. Eng. Chem. 19, 1153–1161. https://doi.org/10.1016/J.JIEC.2012.12.012.

Bağda, E., Sari, A., Tuzen, M., 2018. Effective uranium biosorption by macrofungus (*Russula sanguinea*) from aqueous solution: equilibrium, thermodynamic and kinetic studies. J. Radioanal. Nucl. Chem. 317, 1387–1397. https://doi.org/10.1007/s10967-018-6039-2.

Bağda, E., Tuzen, M., Sarı, A., 2017. Equilibrium, thermodynamic and kinetic investigations for biosorption of uranium with green algae (*Cladophora hutchinsiae*). J. Environ. Radioact. 175–176, 7–14. https://doi.org/10.1016/j.jenvrad.2017.04.004.

Bhat, S.V., Melo, J.S., Chaugule, B.B., D'Souza, S.F., 2008. Biosorption characteristics of uranium(VI) from aqueous medium onto *Catenella repens*, a red alga. J. Hazard Mater. 158, 628–635. https://doi.org/10.1016/J.JHAZMAT.2008.02.042.

Borgatto, F., Dias, C.T.S., Amaral, A.F.C., Melo, M., 2002. Calcium, potassium and magnesium treatment of *Chrysanthemum morifolium* cv. "Bi Time" and callogenesis in vitro. Sci. Agric. 59, 689–693. https://doi.org/10.1590/S0103-90162002000400011.

Brunauer, S., Emmett, P.H., Teller, E., 1938. Adsorption of gases in multimolecular layers. J. Am. Chem. Soc. 60, 309–319. https://doi.org/10.1021/ja01269a023.

Cancian, L.F., Camargo, A.F.M., Silva, G.H.G., 2009. Crescimento de *Pistia stratiotes* em diferentes condições de temperatura e fotoperíodo. Acta Bot. Bras. 23, 552–557. https://doi.org/10.1590/S0102-33062009000200027.

Charles, A.L., Markich, S.J., Ralph, P., 2006. Toxicity of uranium and copper individually, and in combination, to a tropical freshwater macrophyte (*Lemna aequinoctialis*). Chemosphere 62, 1224–1233. https://doi.org/10.1016/J.CHEMOSPHERE.2005.04.089.

Danish, M., Hashim, R., Ibrahim, M.N.M., Rafatullah, M., Sulaiman, O., 2012. Surface characterization and comparative adsorption properties of Cr(VI) on pyrolysed adsorbents of *Acacia mangium* wood and *Phoenix dactylifera* L. stone carbon. J. Anal. Appl. Pyrolysis 97, 19–28. https://doi.org/10.1016/J.JAAP.2012.06.001.

Elangovan, R., Philip, L., Chandraraj, K., 2008. Biosorption of chromium species by aquatic weeds: kinetics and mechanism studies. J. Hazard Mater. 152, 100–112. https://doi.org/10.1016/J.JHAZMAT.2007.06.067.

El-Khaiary, M.I., Malash, G.F., 2011. Common data analysis errors in batch adsorption studies. Hydrometallurgy 105, 314–320. https://doi.org/10.1016/J.HYDROMET.2010.11.005.

Ferreira, R.V.P., Silva, E.A., Canevesi, R.L.S., Ferreira, E.G.A., Taddei, M.H.T., Palmieri, M.C., Silva, F.R.O., Marumo, J.T., 2018. Application of the coconut fiber in radioactive liquid waste treatment. Int. J. Environ. Sci. Technol. 15, 1629–1640. https://doi.org/10.1007/s13762-017-1541-6.

Foo, K.Y., Hameed, B.H., 2010. Insights into the modeling of adsorption isotherm systems. Chem. Eng. J. 156, 2–10. https://doi.org/10.1016/J.CEJ.2009.09.013.

Forzaa, R.C., et al., 2010. Catálogo de plantas e fungos do Brasil, vol. 1 Andrea Jakobsson Estúdio: Instituto de Pesquisas Jardim Botânico do Rio de Janeiro, Rio de Janeiro 2.v.: il.

Fourest, E., Volesky, B., 1996. Contribution of sulfonate groups and alginate to heavy metal biosorption by the dry biomass of *Sargassum fluitans*. Environ. Sci. Technol. 30, 277–282. https://doi.org/10.1021/es950315s.

Gadd, G.M., 2009. Biosorption: critical review of scientific rationale, environmental importance and significance for pollution treatment. J. Chem. Technol. Biotechnol. 84, 13–28. https://doi.org/10.1002/jctb.1999.

Gök, C., Aytas, S., Sezer, H., 2017. Modeling uranium biosorption by *Cystoseira* sp. and application studies. Separ. Sci. Technol. 52, 792–803. https://doi.org/10.1080/01496395.2016.1267212.

Hinz, C., 2001. Description of sorption data with isotherm equations. Geoderma 99, 225–243. https://doi.org/10.1016/S0016-7061(00)00071-9.

Kara, Y., 2012. Bioaccumulation of nickel by aquatic macrophytes. Desalin. Water Treat. 19, 325–328. https://doi.org/10.5004/dwt.2010.1969.

Khani, M.H., 2011. Uranium biosorption by *Padina* sp. algae biomass: kinetics and thermodynamics. Environ. Sci. Pollut. Res. 18, 1593–1605. https://doi.org/10.1007/s11356-011-0518-0.

Khosravi, M., Rakhshaee, R., Ganji, M.T., 2005. Pre-treatment processes of *Azolla filiculoides* to remove Pb(II), Cd(II), Ni(II) and Zn(II) from aqueous solution in the batch and fixed-bed reactors. J. Hazard Mater. 127, 228–237. https://doi.org/10.1016/J.JHAZMAT.2005.07.023.

Kumar, V.K., Sivanesan, S., 2007. Sorption isotherm for safranin onto rice husk: comparison of linear and non-linear methods. Dyes Pigments 72, 130–133. https://doi.org/10.1016/J.DYEPIG.2005.07.020.

Lima, I., Marshall, W.E., 2005. Utilization of Turkey manure as granular activated carbon: physical, chemical and adsorptive properties. Waste Manag. 25, 726–732. https://doi.org/10.1016/J.WASMAN.2004.12.019.

Maine, M.A., Duarte, M.V., Suñé, N.L., 2001. Cadmium uptake by floating macrophytes. Water Res. 35, 2629–2634. https://doi.org/10.1016/S0043-1354(00)00557-1.

Michalak, I., Chojnacka, K., Witek-Krowiak, A., 2013. State of the art for the biosorption process - a review. Appl. Biochem. Biotechnol. 170, 1389–1416. https://doi.org/10.1007/s12010-013-0269-0.

Mkandawire, M., Taubert, B., Dudel, E.G., 2004. Capacity of *Lemna gibba* L. (duckweed) for uranium and arsenic phytoremediation in mine tailing waters. Int. J. Phytoremediation 6, 347–362. https://doi.org/10.1080/16226510490888884.

Mkandawire, M., 2005. Fate and Effect of Uranium and Arsenic in Surface Waters of Abandoned Uranium Mines: Studies with *Lemna gibba* L. Shaker, Aachem. pp. 185.

Oyewo, O.A., Onyango, M.S., Wolkersdorfer, C., 2016. Application of banana peels nanosorbent for the removal of radioactive minerals from real mine water. J. Environ. Radioact. 164, 369–376. https://doi.org/10.1016/J.JENVRAD.2016.08.014.

Panias, D., Krestou, A., 2015. Uranium (VI) speciation diagrams in the $UO_2^{2+}/CO_3^{2-}/H_2O$ system at 25°C. Eur. J. Miner. Process. Environ. Prot. 4 (2).

Pavia, D.L., Lampman, G.M., Kris, G.S., Vyvyan, J.A., 2008. Introduction to Spectroscopy, third ed. Cengage Learning, Washington.

Pratas, J., Paulo, C., Favas, P.J.C., Venkatachalam, P., 2014. Potential of aquatic plants for phytofiltration of uranium-contaminated waters in laboratory conditions. Ecol. Eng. 69, 170–176. https://doi.org/10.1016/J.ECOLENG.2014.03.046.

Ren, G., Hu, D., Cheng, E.W.C., Vargas-Reus, M.A., Reip, P., Allaker, R.P., 2009. Characterisation of copper oxide nanoparticles for antimicrobial applications. Int. J. Antimicrob. Agents 33, 587–590. https://doi.org/10.1016/J.IJANTIMICAG.2008.12.004.

Saleh, T.A., Naeemullah, Tuzen, M., Sarı, A., 2017. Polyethylenimine modified activated carbon as novel magnetic adsorbent for the removal of uranium from aqueous solution. Chem. Eng. Res. Des. 117, 218–227. https://doi.org/10.1016/j.cherd.2016.10.030.

Salman, A., Tsror, L., Pomerantz, A., Moreh, R., Mordechai, S., Huleihel, M., 2010. FTIR spectroscopy for detection and identification of fungal phytopathogenes. Spectroscopy 24, 261–267. https://doi.org/10.3233/SPE-2010-0448.

Sar, P., D'Souza, S.F., 2001. Biosorptive uranium uptake by a *Pseudomonas* strain: characterization and equilibrium studies. J. Chem. Technol. Biotechnol. 76, 1286–1294. https://doi.org/10.1002/jctb.517.

Sari, A., Mendil, D., Tuzen, M., Soylak, M., 2008. Biosorption of Cd(II) and Cr(III) from aqueous solution by moss (*Hylocomium splendens*) biomass: equilibrium, kinetic and thermodynamic studies. Chem. Eng. J. 144, 1–9. https://doi.org/10.1016/j.cej.2007.12.020.

Sari, A., Tuzen, M., 2008. Biosorption of total chromium from aqueous solution by red algae (*Ceramium virgatum*): equilibrium, kinetic and thermodynamic studies. J. Hazard Mater. 160, 349–355. https://doi.org/10.1016/j.jhazmat.2008.03.005.

Sari, A., Tuzen, M., 2009. Removal of mercury(II) from aqueous solution using moss (*Drepanocladus revolvens*) biomass: equilibrium, thermodynamic and kinetic studies. J. Hazard Mater. 171, 500–507. https://doi.org/10.1016/j.jhazmat.2009.06.023.

Sheppard, S.C., Sheppard, M.I., Gallerand, M.O., Sanipelli, B., 2005. Derivation of ecotoxicity thresholds for uranium. J. Environ. Radioact. 79, 55–83. https://doi.org/10.1016/j.jenvrad.2004.05.015.

Skillicorn, P., Spira, W., Journey, W., 1993. Duckweed Aquaculture: a New Aquatic Farming System for Developing Countries.

Tavares, F.A., 2004. Eficiência da *Lemna* sp. no tratamento de efluentes líquidos de suinocultura e sua utilização como fonte alternativa de alimento para tilápias. https://doi.org/10.13140/RG.2.1.3830.6962.

Tuzen, M., Dogan, M., Uluozlu, O.D., Mendil, D., Sarı, A., Soylak, M., 2008. Characterization of biosorption process of As(III) on green algae *Ulothrix cylindricum*. J. Hazard Mater. 165, 566–572. https://doi.org/10.1016/j.jhazmat.2008.10.020.

Uluozlu, O.D., Sari, A., Tuzen, M., Soylak, M., 2008. Biosorption of Pb(II) and Cr(III) from aqueous solution by lichen (*Parmelina tiliaceae*) biomass. Bioresour. Technol. 99, 2972–2980. https://doi.org/10.1016/j.biortech.2007.06.052.

Umali, L.J., Duncan, J.R., Burgess, J.E., 2006. Performance of dead *Azolla filiculoides* biomass in biosorption of Au from wastewater. Biotechnol. Lett. 28, 45–50. https://doi.org/10.1007/s10529-005-9686-7.

Vilar, V.J.P., Botelho, C.M.S., Boaventura, R.A.R., 2007. Methylene blue adsorption by algal biomass based materials: biosorbents characterization and process behaviour. J. Hazard Mater. 147, 120–132. https://doi.org/10.1016/j.jhazmat.2006.12.055.

Volesky, B., 2003. Sorption and Biosorption, first ed. BV Sorbex, Montreal, Canada 2003.

Volesky, B., 1987. Biosorbents for metal recovery. Trends Biotechnol. 5, 96–101. https://doi.org/10.1016/0167-7799(87)90027-8.

Volk, G.M., Goss, L.J., Franceschi, V.R., 2004. Calcium channels are involved in calcium oxalate crystal formation in specialized cells of *Pistia stratiotes* L. Ann. Bot. 93, 741–753. https://doi.org/10.1093/aob/mch092.

Wang, J., song, Hu, jiang, X., Wang, J., Bao, Z., lei, Xie, Yang, S bo, hui, J., 2010. The tolerance of *Rhizopus arrihizus* to U(VI) and biosorption behavior of U(VI) onto *R. arrihizus*. Biochem. Eng. J. 51, 19–23. https://doi.org/10.1016/j.bej.2010.04.010.

Yang, J., Volesky, B., 1999. Biosorption of uranium on Sargassum biomass. Water Res. 33, 3357–3363. https://doi.org/10.1016/S0043-1354(99)00043-3.

Yi, Z., Yao, J., Chen, H., Wang, F., Yuan, Z., Liu, X., 2016. Uranium biosorption from aqueous solution onto *Eichhornia crassipes*. J. Environ. Radioact. 154, 43–51. https://doi.org/10.1016/J.JENVRAD.2016.01.012.

Zelentsov, V., Datsko, T., Dvornikova, E., 2012. Adsorption models for treatment of experimental data on removal fluorine from water by oxihydroxides of aluminum. Rom. Soc. Ind. Appl. Math. J. 8, 209–215.